Pergamon

Cement and Concrete Research, Vol. 26, No. 4, pp. 557-565, 1996

0008-8846/96 $15.00 + .00

PII S0008-8846(96)00034-8

DURABILITY OF HIGH PERFORMANCE CONCRETE IN MAGNESIUM BRINE

Peter J. Tumidajski and G.W. Chan
Materials Laboratory, Institute for Research in Construction
National Research Council of Canada
Ottawa, Ontario, Canada K1A 0R6

(Refereed)
(Received August 21, 1995; in final form February 12, 1996)

ABSTRACT

The durability of six concretes exposed to magnesium brine was monitored for 24 months. These concretes incorporated ground granulated blast furnace slag, silica fume, and fly ash. The Young's moduli, chloride penetrations, and median pore diameters were measured. There was a cyclic nature to these properties due to the complicated interaction of hydration with magnesium, chloride and sulfate attack. Mineral admixtures, in combination with a long initial cure, provided the most durable concrete. Concrete with 65% slag had the best overall durability to the brines tested.

Introduction

Concrete is exposed to high-concentration magnesium brine in structures built for seawater or groundwater service, and in facilities which process magnesium brine producing high value-added end products (e.g. potash mills). Exposure to magnesium brine compromises the expected service life of the structure by a combination of the following (1–8):

- Calcium dissolution by the magnesium cation,

$$Mg^{2+} + Ca(OH)_2 \leftrightarrow Mg(OH)_2 + Ca^{2+}$$

  The $Mg(OH)_2$ is almost insoluble and shifts the equilibrium to the right which depletes the $Ca(OH)_2$ in the hydrated cement phase. Additionally, there are tensile stresses associated with the formation of $Mg(OH)_2$ because the molar volume of $Mg(OH)_2$ exceeds that of $Ca(OH)_2$. The concrete will crack when the tensile strength of the hydrated cement phase is exceeded. Consequently, the concrete becomes more permeable.
- Reaction of $Mg(OH)_2$ with chloride forming magnesium hydroxychloride ($Mg_2(OH)_3Cl.4H_2O$).
- Magnesium substitution for calcium in the calcium-silicate-hydrate (C-S-H) eventually forming non-cementitious magnesium-silicate-hydrate (M-S-H).
- Reaction of sulfate and chloride in the brine with the hydrated aluminate or $Ca(OH)_2$ phases forming calcium-sulfo-aluminate ($3CaO.Al_2O_3.CaSO_4.12H_2O$) and calcium-chloro-aluminate ($3CaO.CaCl_2.10H_2O$). The latter both eventually convert to expansive ettringite ($3CaO.Al_2O_3.3CaSO_4.32H_2O$).

TABLE 1

Nomenclature and Composition of Systems*

	Type 10 Cement (%)	Type 50 Cement (%)	Slag (%)	Fly Ash (%)	Silica Fume (%)	Curing Time (days)
System B	0	100	0	0	0	3 & 28
System C	52	0	45	0	3	3 & 28
System D	40	0	55	0	5	3 & 28
System E	32	0	65	0	3	3 & 28
System F	22	0	75	0	3	3 & 28
System G	42	0	0	58	0	28

*CSA Type 10 and 50 are identical to ASTM Type 1 and V, respectively.

TABLE 2

Chemical Composition of Cement, Silica Fume, Fly Ash and Blast Furnace Slag

(%)	Type 10 Cement	Type 50 Cement	Silica Fume	Fly Ash	Slag
SiO_2	21.39	23.18	95.17	53.90	39.67
Al_2O_3	5.26	5.19	0.21	20.90	6.90
Fe_2O_3	2.07	4.12	0.13	3.52	1.48
CaO	66.35	56.77	0.23	12.00	35.68
MgO	1.55	3.64	0.15	1.11	12.93
Na_2O	0.09	1.08	0.10	2.74	0.18
K_2O	1.00	0.52	0.27	0.50	0.29
C	-	-	1.56	-	-
L-O-I*	0.35	2.39	2.30	0.57	0.56
SO_3	1.42	2.75	0.12	0.09	3.23
Free Lime	0.94	0.47	-	-	-

*Loss on ignition.

TABLE 3

Proportions (kg/m^3) for the Concrete Systems

	System B	System C	System D	System E	System F	System G
Cement	370	192	1478	118	81.4	157
Slag	0	166	203	240	277	0
Fly Ash	0	0	0	0	0	215
Silica Fume	0	11.1	18.5	11.1	11.1	0
Water	148	148	148	148	148	115
Coarse Aggregate	1107	1107	1107	1107	1107	1249
Fine Aggregate	738	738	738	738	738	606
Air Agent	0.9	0.9	0.9	0.9	0.9	0.6
Superplasticizer	4.6	4.6	4.6	5.0	4.6	5.1
Accelerator		3.7	3.7	3.7	3.7	3.7
Slump (*mm*)	114	114	165	140	152	114
Air (%)	5.0	4.8	5.5	4.0	5.0	4.0

- Decomposition of the C-S-H phase because the magnesium brine lowers the $(OH)^-$ activity of the porewater to such an extent that the C-S-H is no longer thermodynamically stable.

Durability studies of the interaction of magnesium brine with concrete have almost exclusively been limited to ordinary Portland cement concrete and synthetic brine. Recently, the durability of blended cement concrete exposed to natural magnesium brine was reported. In the first

TABLE 4

Ion Concentrations of Brines (%)

	Brine 1	Brine 2
K^+	4.68	4.32
Cl^-	16.82	16.98
SO_4^{2-}	0.18	0.16
Ca^{2+}	0.134	0.154
Mg^{2+}	0.107	1.46
Na^+	7.76	5.44

case, a 30% fly ash concrete was exposed to groundwater with an extremely high magnesium content (1,9). After six years of exposure, there was severe deterioration. In the second case, 15% silica fume concrete was exposed to Dead Sea brine (10). In contrast to the earlier work of Feldman and Cheng-yi (11), the silica fume was ineffective in preventing degradation.

Despite encouraging results on the durability of ground granulated blast furnace slag and cement mortars exposed to brine (12), nothing has been reported in the literature for the corresponding concretes. Concrete mixtures incorporating slag are believed to be especially suitable for resisting magnesium attack because of decreased permeabilities and low $Ca(OH)_2$ contents. Therefore, it was the object of this investigation to evaluate the durability of several blended cement concretes to brines with variable magnesium content. The experimental concretes incorporated ground granulated blast furnace slag and high volume fly ash and were compared to the durability of a Type 50 sulfate-resistant cement concrete control.

Experimental

Six concrete mixtures were proportioned using cements and cement blends as listed in Table 1. The chemical composition of the cements, the silica fume, fly ash and ground granulated blast furnace slag are presented in Table 2. The proportions for the six concrete systems are in Table 3. The coarse aggregate was crushed limestone (< 19 *mm*), and graded silica sand was the fine aggregate. The air entraining agent was Darex, and the superplasticizer was a 40% Disal solution. The chemical, Na_2SO_4, was added as an accelerating agent. The slump and the entrained air for each mix design are reported in Table 3.

All concrete was cured at 100% *rh* for the times indicated in Table 1. At the conclusion of curing, the compressive strengths (ASTM C39-86), rapid chloride permeabilities (ASTM C1202-91), $Ca(OH)_2$ content and non-evaporable water (Thermal gravimetric analysis) and porosities/pore size distributions (mercury intrusion) were determined. Two beam geometries were required for the brine exposure experiments. For chloride ingress measurements, beams of dimension 75 *mm* × 75 *mm* × 300 *mm* were used. The beams were waxed on five sides and immersed in two brines. The composition of the brines is given in Table 4. At 3, 6, 12, 18 and 24 months, the beams were removed from the baths. The 0.1% chloride front was determined by measuring total chloride (ASTM C114) at various penetration depths from the unwaxed specimen surface. The porosities and pore size distributions by mercury intrusion were determined on the mortar portion of the concrete at a depth of 4 *mm* from the surface. Flat beams of dimension 25 *mm* × 75 *mm* × 300 *mm* were used to non-destructively monitor the change in Young's modulis (ASTM C78-84) during exposure to the brines. A minimum of five specimens was used to calculate the averaged Young's modulis for each experimental condition.

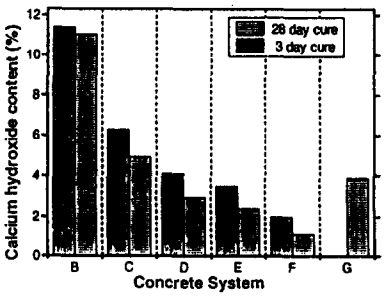

FIG. 1.
Calcium hydroxide contents for the concrete systems.

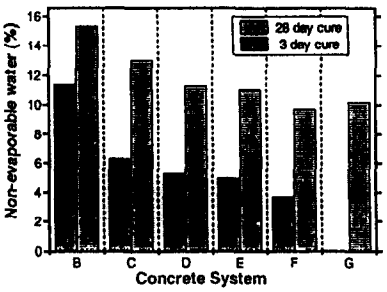

FIG. 2.
Non-evaporable water contents for the concrete systems.

Results and Discussion

The $Ca(OH)_2$ content and non-evaporable water for all systems are presented in Figures 1 and 2, respectively. Clearly, curing for more than three days is necessary for the slag blends. For example, the non-evaporable water for System D increases from 5.3% to 11.3 % while the $Ca(OH)_2$ content decreases from 4.1% to 3.0%. In contrast, changes in the System B control are not major between 3 and 28 days curing periods.

Compressive strength values are presented in Figure 3. After 3 days curing, System B displays the highest strength, followed by System C and E and then systems D and F. After 28 days of curing, System G (high volume fly ash) has the greatest strength, followed by System E. Systems B, D, F and C follow and are similar. The contrast in the effect of curing time on the slag systems and the Type 50 control is evident.

Results of the rapid chloride permeability test on Systems B to G for both curing conditions are presented in Figure 4. The value for the accumulated charge passed in six hours, is lowest for System F at both 3 and 28 days of curing. The value for System B is considerably greater than the other systems after 28 days of curing, and is also quite large after 3 days of curing. By comparing Figures 3 and 4, it is seen that compressive strength is a poor indicator of results from the rapid chloride permeability test.

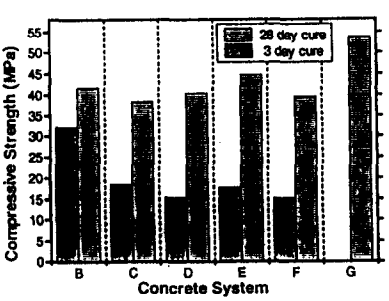

FIG. 3.
Compressive strengths for the concrete systems.

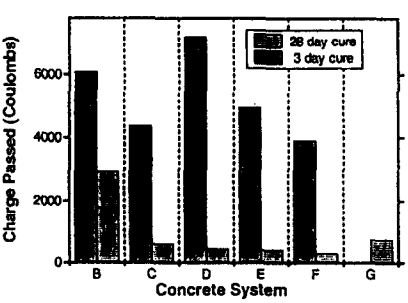

FIG. 4.
Total charge accumulated during rapid chloride permeability test.

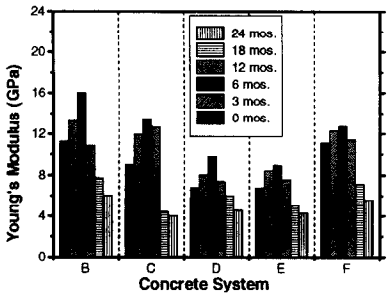

FIG. 5.
Young's moduli for concrete systems cured for 3 days and exposed to brine 1.

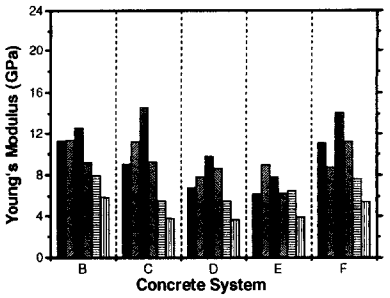

FIG. 6.
Young's moduli for concrete systems cured for 3 days and exposed to brine 2. Length of exposure defined in Figure 5.

Mechanical deterioration of the concrete due to exposure to the brines was monitored by Young's moduli measurements. The results for 24 months exposure are presented in Figures 5 and 6 for concrete cured for 3 days and subjected to brines 1 and 2, respectively, and in Figures 7 and 8 for concrete cured for 28 days and subjected to brines 1 and 2 respectively. There are several global trends. Irrespective of the length of curing and mix design, specimens exposed to the higher magnesium content (brine 2) always developed a lower maximum Young's moduli, and the Young's moduli always decayed quicker than the concrete exposed to the lower magnesium content brine 1. The observation adds to the evidence that magnesium directly attacks the hydrated cement phase and weakens the concrete. Regardless of the mix design, longer curing produces a concrete with a higher Young's moduli. Furthermore, for many of the 3 day cured specimens, the Young's moduli increased up to 12 months and then decreased suggesting that the hydration which continued in the presence of the brine was affected. For the 28 day cured specimens, the Young's moduli of the concrete was essentially constant until 12 months and then decreased. In well cured concrete, brine attack is impeded by the low permeability of the concrete. For 28 day cured concrete, all systems exhibited mech-

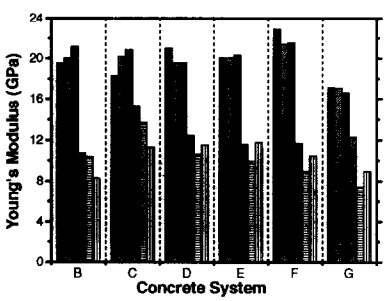

FIG. 7.
Young's moduli for concrete systems cured for 28 days and exposed to brine 1. Length of exposure defined in Figure 5.

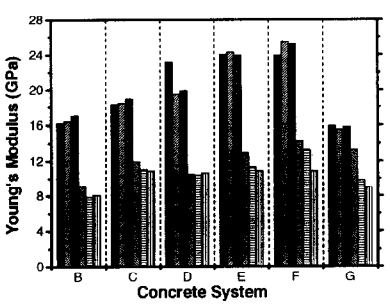

FIG. 8.
Young's moduli for concrete systems cured for 28 days and exposed to brine 2. Length of exposure defined in Figure 5.

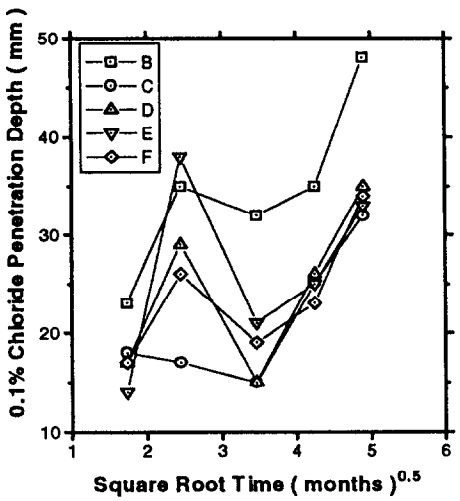

FIG. 9.
Chloride penetration front versus time for concrete systems cured for 3 days and exposed to brine 1.

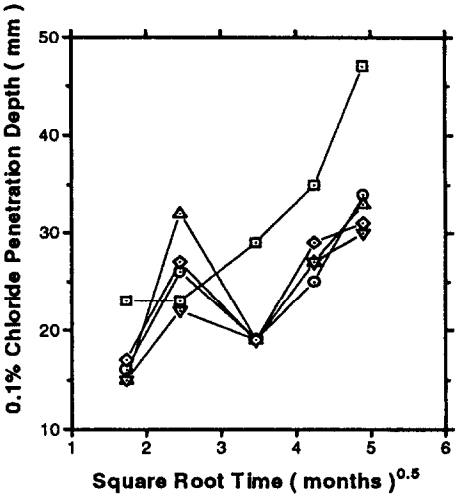

FIG. 10.
Chloride penetration front versus time for concrete systems cured for 3 days and exposed to brine 2. Symbols defined in Figure 9.

anical degradation but System E appears to have a slightly greater resistance to mechanical degradation albeit the other slag systems (Systems C, D, and F) are comparable. System B recorded the largest degradation in Young's moduli. System G was intermediate between the best and worst cases.

The 0.1% chloride penetration fronts for 24 months exposure to the brines are presented in Figures 9 and 10 for concrete cured for 3 days and exposed to brines 1 and 2 respectively, and in Figures 11 and 12 for concrete cured for 28 days and exposed to brines 1 and 2 respectively. All the 3 day cured slag specimens (Systems C, D, E and F) showed an increase in the 0.10% chloride front at 18 and 24 months of exposure to both brines 1 and 2. However, the increase followed a sharp decrease in chloride penetration at 12 months. The same phenomenon occurred for System G. It appears that the behavior occurs with mix designs which are slow in hydrating (i.e. the slag and high volume fly ash concretes). Consequently, the hydration, magnesium, chloride and sulfate reactions occur simultaneously. It is believed that extra reaction products are formed in and block the pores nearer the surface. This creates a front which is less permeable than the normal reaction products. Alternatively, a less permeable product forms due to the hydration reaction in the presence of the magnesium, chloride and sulfate ions in the brine. Consequently, less chloride enters deeper into the specimen resulting in a reduction in chloride beneath the layer which is observed at 12 months. Subsequent further reaction in the surface layer at 18 and 24 months either cracks the concrete which allows further chloride ingress or the initial layers of hydration products are directly attacked by the brine. The phenomenon is less pronounced for concrete incorporating slag and cured for 28 days because the concrete is well hydrated and has developed a less permeable structure. Additionally, well hydrated concretes incorporating slag will have much less $Ca(OH)_2$; therefore they are less susceptible to deleterious $Mg(OH)_2$ formation. In all cases, the blended cement concretes offer greatly improved resistance to chloride penetration over the System B control concrete. System

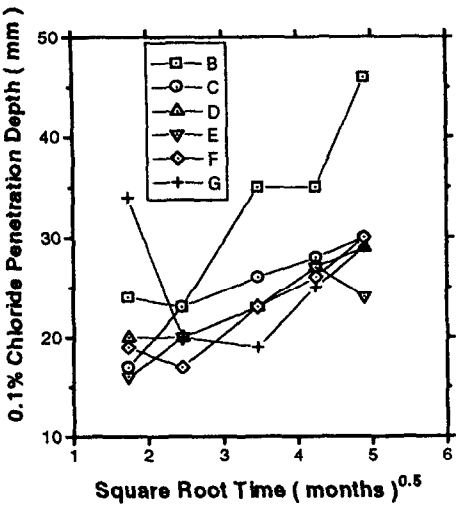

FIG. 11.
Chloride penetration front versus time for concrete systems cured for 28 days and exposed to brine 1.

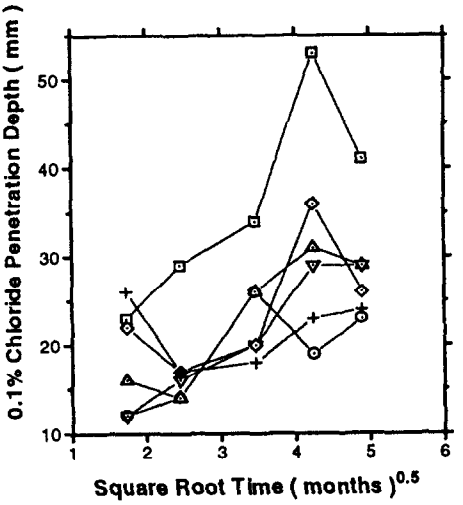

FIG. 12.
Chloride penetration front versus time for concrete systems cured for 28 days and exposed to brine 2. Symbols defined in Figure 11.

E generally shows the least chloride ingress irrespective of curing or exposure conditions. The plots given in Figures 9 to 12 are non-linear especially for the early exposure times. This result suggests that chloride penetration from brine is a combination of diffusion and chemical reaction.

The median pore diameter of test concretes at times up to 24 months exposure to the brines are presented in Figures 13 and 14 for concrete cured for 3 days and exposed to brines 1 and 2 respectively, and Figures 15 and 16 for concrete cured for 28 days and exposed to brines 1 and 2 respectively. The median pore diameter for concrete cured for 3 days is generally larger when exposed to the high magnesium content brine 2 confirming that magnesium chloride

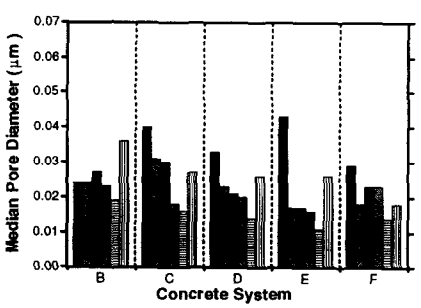

FIG. 13
Median pore diameter for concrete systems cured for 3 days and exposed to brine 1. Length of exposure defined in Figure 5.

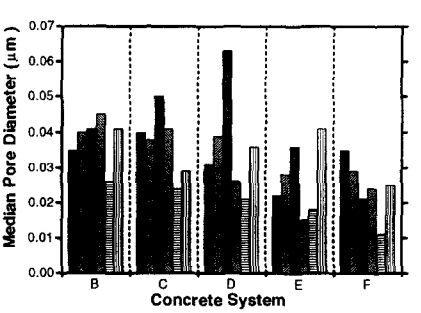

FIG. 14.
Median pore diameter for concrete systems cured for 3 days and exposed to brine 2. Length of exposure defined in Figure 5.

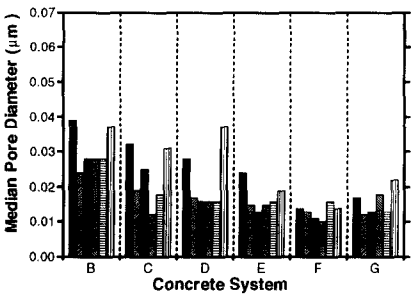

FIG. 15.
Median pore diameter for concrete systems cured for 28 days and exposed to brine 1. Length of exposure defined in Figure 5.

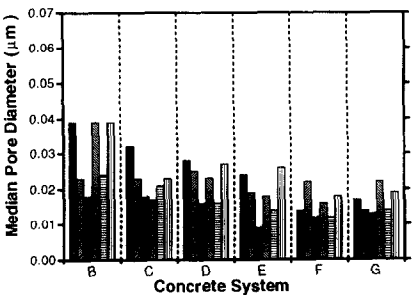

FIG. 16.
Median pore diameter for concrete systems cured for 28 days and exposed to brine 2. Length of exposure defined in Figure 5.

alters and subsequently opens the microstructure (7). As expected, for 28 day cured concrete, the influence of the higher magnesium content is not as pronounced because the concrete is less permeable. For exposure to brine 1 and with respect to curing time, longer curing time produces initially a smaller median pore diameter, as expected. But, the median pore diameter develops a cyclic nature. The median pore diameter decreases to a minimum value at about 12 months. Subsequently, the median pore diameter increases in value. For concrete cured for 3 days and exposed to the high magnesium content brine 2, all concrete systems except System F reached a maximum in the median pore diameter after 6–12 months exposure. Subsequently, the values for the median pore diameter dropped and again increased at 24 months. For System F, there was a gradual decrease in the median pore diameter to a minimum median pore diameter at 18 months then a sharp rise in the median pore diameter value 24 months. It may be that there is a competition between $MgCl_2$ and $MgSO_4$ attack and the resultant microstructure. In the former case, the microstructure is opened by the reaction products while in the latter case the microstructure is plugged with reaction products (2,4,6,7,9). Alternately, a simpler explanation for the cyclic nature in the microstructural descriptors may be given. During $MgSO_4$ attack, the surface layers become soft. These layers may disintegrate or partially dissolve in the surrounding brine. This exposes a layer underneath which is in better condition. Whatever the mechanism, it is clear that concretes incorporating higher slag contents (System E or F) and fly ash (System G) consistently recorded the lowest median pore diameters after extended brine exposure.

Conclusions

- The combination of hydration of the cement phases with ingress of the aggressive ions in concrete exposed to brine leads to the development of a cyclic nature for the Young's moduli, chloride penetrations, and microstructural descriptors.
- A long initial cure in conjunction with blended cement concretes incorporating mineral admixtures provides the best protection from brine.
- All systems exhibited degradation in the presence of the brines. However, System E (32% Type 10 cement, 65% slag and 3% silica fume) with 28 days hydration had the lowest overall rate of degradation and the best overall durability to brine.

Acknowledgment

Financial assistance from the Saskatchewan Potash Producers Association is gratefully acknowledged.

References

1. L.D. Wakeley, T.S. Poole, C.A. Weiss and J.P. Burkes, *Geochemical Stability of Cement Based Composites in Magnesium Brines*, Proceedings of the Fourteenth International Conference on Cement Microscopy, April 5–9 (1992), Costa Mesa, California, International Cement Microscopy Association, pp. 333–350.
2. C. Ftikos and G. Parissakis, *The Combined Action of Mg^{2+} and Cl^- Ions in Cement Pastes*, Cement and Concrete Research **15**, 593–599 (1985).
3. I.M. Helmy, A.A. Amer and H. El-Didamony, *Chemical Attack on Hardened Pastes of Blended Cements, Part I: Attack of Chloride Ions*, Zement-Kalk-Gipps, No. 1, 46–50 (1991).
4. R. Oberste-Padtberg, *Degradation of Cements by Magnesium Brines*, Proceedings of the Seventh International Conference on Cement Microscopy, March 25–28 (1985), Forth Worth, Texas, International Cement Microscopy Association, pp. 24–36.
5. M. Regourd, M. Hornani and B. Montureux, *Microstructure of Concrete in Aggressive Environments*, Edited by P. Sereda and J. Litvan, ASTM STP 691, 253–268 (1978).
6. D. Bonen and M.D. Cohen, *Magnesium Sulfate Attack on Portland Cement Paste, Part I: Microstructural Analysis*, Cement and Concrete Research **22**, 169–180 (1992).
7. M. Moukwa, *Characteristics of the Attack of Cement Paste by $MgSO_4$ and $MgCl_2$ from the Pore Structure Measurements*, Cement and Concrete Research **20**, 148–158 (1990).
8. R.S. Gollop and H.F.W. Taylor, *Microstructural and Microanalytical Studies of Sulfate Attack. Part I: Ordinary Portland Cement Paste*, Cement and Concrete Research **22**, 1027–1038 (1992).
9. L.D. Wakeley, T.S. Poole and J. P. Burkes, Alteration of Concrete by Magnesium Brine, Paper presented at the American Concrete Institute Symposium of Committee 227 on Concrete for Radioactive Disposal, March 17–21 (1991), Boston, MA.
10. A. Bentur and M. Ben-Bassat, *Durability of High Performance Concretes in Highly Concentrated Magnesium Solutions*, In Proceedings of the International Conference on Durability of Building Materials and Components 6, Edited by S. Nagataki, T. Nireki and F. Tomosawa, Japan (1992), E.& FN Spon.
11. R.F. Feldman and H. Cheng-yi, *Resistance of Mortars Containing Silica Fume to Attack by a Solution Containing Chlorides*, Cement and Concrete Research **15**, 411–420 (1985).
12. R.F. Feldman and V.S. Ramachandran, *New Accelerated Methods for Predicting Durability of Cementitious Materials*, Edited by P. Sereda and J. Litvan, ASTM STP 691, 313–325 (1978).